Photophysical Properties of Mono- and Multiply-Functionalized Fullerene Derivatives

Dirk M. Guldi* and Klaus-Dieter Asmus*

Radiation Laboratory and Department of Chemistry and Biochemistry, University of Notre Dame,
Notre Dame, Indiana 46656

Received: October 29, 1996; In Final Form: December 12, 1996[⊗]

Time-resolved and steady-state techniques have been performed to investigate the photophysical properties of $C_{60}[C(COOEt)_2]$ (**Ia**), *e*-$C_{60}[COOEt)_2]_2$ (**IIa**) (*e* = equatorial), *trans*-3-$C_{60}[C(COOEt)_2]_2$ (**IIb**), *trans*-2-$C_{60}[C(COOEt)_2]_2$ (**IIc**), and *e,e,e*-$C_{60}[C(COOEt)_2]_3$ (**III**) (*e* = equatorial). Picosecond-resolved energy transfer to the fullerene core results in the rapid formation of the excited singlet state with remarkably blue-shifted singlet−singlet ($S^*_1 \rightarrow S^*_n$) transitions (868 nm (**III**)) relative to pristine C_{60} (920 nm). Intersystem crossing to the energetically lower lying excited triplet state exhibits a deceleration with increasing number of functionalizing addends. The corresponding triplet−triplet ($T^*_1 \rightarrow T^*_n$) absorption energies also show a significant dependence on the degree and site of functionalization, spreading over a range of 100 nm (750 nm for $^3C_{60}$ to 650 nm for *e,e,e*-$(^3C_{60})[C(COOEt)_2]_3$ (**III**)). Energy transfer from radiolytically excited biphenyl (^{3}BP) to the fullerene's ground state corroborates the photolytic data. $*0 \rightarrow 0$ Emissions from the lowest level of the excited singlet state (fluorescence) are mirror images of the reversed $0 \rightarrow *0$ absorption transitions with minor Stokes shift. Red shifts of fluorescence- and phosphorescence-related emission, relative to pristine C_{60}, again sensitively reflect the perturbation of the fullerene's π-system as a function of the degree and site of functionalization. Cyclic voltammetry and reductive quenching of excited triplet fullerenes demonstrate that functionalization of C_{60} obstructs the ease of reduction in the ground and excited triplet state. An increasing number of functional groups results in a cathodic shift of the redox potential (ground state −0.54 to −0.86 V; excited singlet state 1.44 to 0.91 V; excited triplet state +1.01 to +0.64 V *versus* SCE for C_{60} and *e,e,e*-$(^3C_{60})[C(COOEt)_2]_3$ (**III**), respectively).

Introduction

The unique reactivity and the predominantly hydrophobic nature of buckmimsterfullerene, C_{60}, stimulated broad and interdisciplinary interest to modfy its polyfunctional structure, which contains 30 reactive double bonds located at the junctions of two hexagons via an extended number of addition reactions.[1] The various types of functionalized fullerene derivatives so far synthesized include (i) cyclic adducts formed via cycloaddition,[2] (ii) $C_{60}-R_x$ type of derivatives resulting from radical addition or by reaction of $C_{60}{}^{n-}$ anions with various alkyl halides,[3] (iii) adducts involving triangular bridging of a C−C bond,[4] and (iv) organometallic derivatives.[5] Covalent attachment of a large number of addends at the hydrophobic fullerene core has been shown to lead to novel and innovative materials with unique properties ranging from drug delivery to advanced nanostructured devices.[6]

The most intriguing functionalized fullerene derivatives comprise photo-/electroactive donor−bridge−acceptor dyads[7] or hydrophilic/amphiphilic suprastructures.[8] In fullerene/ferrocene-based multicomponent supramolecular assemblies, C_{60} has been demonstrated to operate as a photosensitive unit undergoing rapid intramolecular electron transfer reactions.[2e] Evidence for photoinduced intramolecular electron and energy transfer was found in a ruthenium(II) tris(bipyridine) donor−bridge−acceptor dyad, one of the most prominent examples of a chromophore donor or acceptor unit synthetically bound to the fullerene core.[9] Only a few recent reports, despite considerable efforts, have appeared on the unequivocal formation of stable monolayers and multilayers from amphiphilic C_{60} derivatives.[10] Well-organized two- and three-dimensional networks are an essential requirement for the construction of fullerene-based nanostructured devices. Water-soluble derivatives even appear to exhibit biological benefits such as antiviral activity, e.g. in connection with HIV.[11]

One approach to studying photophysical properties of derivatized fullerenes focuses on photo-/electroinactive functionalization, e.g. by a bis(ethoxycarbonyl)methylene group in a 6-6 closed-adduct.[4a−d] Functionalization of a C=C double bond, located at a junction of two hexagons, basically sustains the fullerene structure. The reduction of symmetry in monoadducts results, however, in a regioselectivity of subsequent functionalization reactions at specific positions. This reveals that some bonds in the functionalized fullerene become preactivated, leading to a preferential substitution at certain C=C double bonds. Hence, the first step in the synthesis is the formation of a monoadduct, e.g. $C_{60}[C(COOEt)_2]$ (**Ia**), which upon further addition is successively transformed into well-defined bis- and tris-regioisomers, $C_{60}[C(COOEt)_2]_n$ ($n = 2, 3$) (**II**, **III**).

Once synthesized, many of the functionalized fullerene derivatives have been subjects of photochemical, photophysical,[7f,12] and electrochemical studies.[13] Relevant information has, in particular, been published for monofunctionalized systems, while only little quantitative information is available so far regarding multiply-functionalized derivatives.

A particularly sensitive set of parameters to study the electronic properties of fullerenes are optical absorption and emission spectra. Fluorescence from excited singlet C_{60} and some functionalized fullerene derivatives has been reported at room temperature and in frozen matrix (77 K),[14] although the fluorescence-related emission of C_{60} is still a matter of controversial discussion. Phosphorescence from excited triplet C_{60} furthermore reveals, for example, weak radiative transitions between states of different multiplicity.[15]

[⊗] Abstract published in *Advance ACS Abstracts,* February 1, 1997.

S1089-5639(96)03355-5 CCC: $14.00

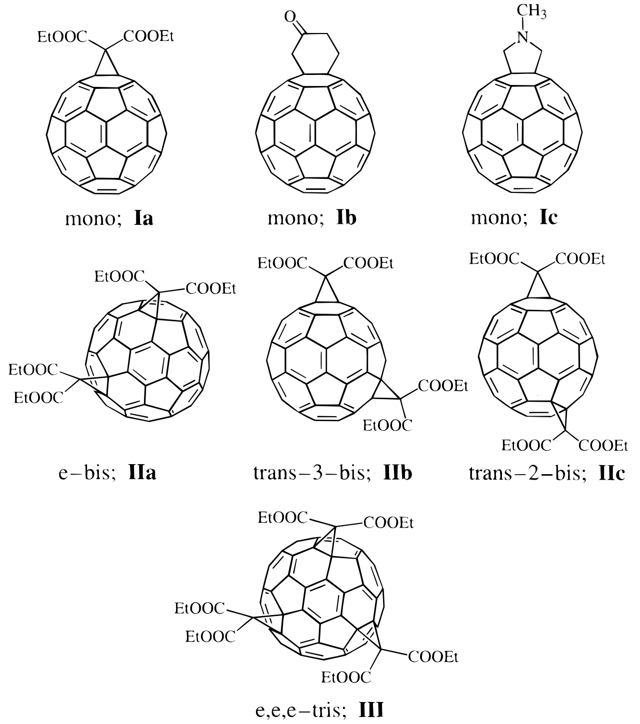

Figure 1. Compounds used in this study.

The present detailed investigation on mono- and multiply-functionalized C_{60} demonstrates, for the first time, the impact of single and multiple addends on the photophysical and redox properties of the fullerene's ground and photoexcited state, by means of employing time-resolved and steady-state techniques. Furthermore, compilation of the photophysical and electrochemical parameters resulted in a more qualitative interpretation of the quenching rates.

Experimental Section

Details of the synthesis of the mono- and multiply-functionalized fullerenes (for structural details see Figure 1) are described in earlier contributions.[2b,4a,b,12a] All organic solvents were redistilled prior to use.

Picosecond Laser Flash Photolysis. Picosecond laser flash photolysis experiments were carried out with 532-nm laser pulses from a mode-locked, Q-switched Quantel YG-501 DP Nd:YAG laser system (pulse width ≈ 18 ps, 2−3 mJ/pulse). The white continuum picosecond probe pulse was generated by passing the fundamental output through a D_2O/H_2O solution. The excitation and the probe were fed to a spectrograph (HR-320, ISDA Instruments, Inc.) with fiber-optic cables and were analyzed with a dual diode array detector (Princeton Instruments, Inc.) interfaced with an IBM-AT computer. The details of the experimental setup and its operation have been described elsewhere.[16]

Nanosecond Laser Flash Photolysis. These experiments were performed with laser pulses from a Quanta-Ray CDR Nd: YAG system (532 nm, 6-ns pulse width, 5−10 mJ/pulse) in a front face excitation geometry. Alternatively, excitation experiments were performed with laser pulses from a Molectron UV-400 nitrogen laser system (337.1 nm, 8-ns pulse width, 1 mJ/pulse). The photomultiplier output was digitized with a Tektronix 7912 AD programmable digitizer. A typical experiment consisted of 5−10 replicate pulses per measurement. The averaged signal was processed with an LSI-11 microprocessor interfaced with a VAX-370 computer. Details of the experimental setup can be found elsewhere.[17]

Pulse Radiolysis. Pulse radiolysis experiments were performed by utilizing 50-ns pulses of 8-MeV electrons from a Model TB-8/16-1S electron linear accelerator. Basic details of the equipment and the data analysis have been described elsewhere.[18] Dosimetry was based on the oxidation of SCN^- to $(SCN)_2^{\bullet -}$, which in aqueous, N_2O-saturated solutions takes place with $G \approx 6$ (G denotes the number of species per 100 eV, or the approximate micromolar concentration per 10 J of absorbed energy). The radical concentration generated per pulse amounts to $(1-3) \times 10^{-6}$ M for all the systems investigated in this study.

Absorption spectra were recorded with a Milton Roy Spectronic 3000 Array spectrophotometer.

Emission spectra were recorded with a SLM 8100 spectrofluorometer. Fluorescence spectra were measured in methylcyclohexane solutions containing 10^{-4} M fullerene, forming clear, noncracking glasses in liquid N_2. A 570-nm long-pass filter in the emission path was used in order to eliminate the interference from the solvent and stray light. No correction were performed for the fluorescence and phosphorescence, but long integration times (20 s) and low increments (0.1 nm) were applied. The slits were 2 and 8 nm, and each spectrum was an average of at least five individual scans.

Cyclic voltammetry measurements were performed with a glassy carbon electron, polished with a 1 μm diamond paste before each run, a Pt counter electrode, and an aqueous standard calomel electrode as reference. All potential values cited within this paper are *versus* SCE. The experimental setup was described earlier.[12b] The scan rate was varied between 25 and 500 mV/s. If not specifically noted, the experiments were conducted at 50 mV/s.

All experiments were carried out at room temperature, 22 ± 2 °C. Experimental error limits are estimated to be ±10% unless otherwise noted.

Results and Discussion

The general processes involved in the photochemistry of excited fullerenes are summarized in Chart 1.[19] Since the bis(ethoxycarbonyl)methylene group lacks any photo- and electroactivity, it is feasible to assume similar photochemical

CHART 1

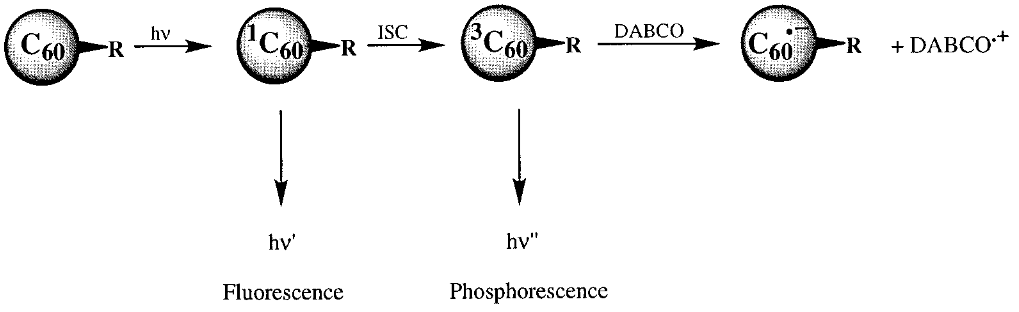

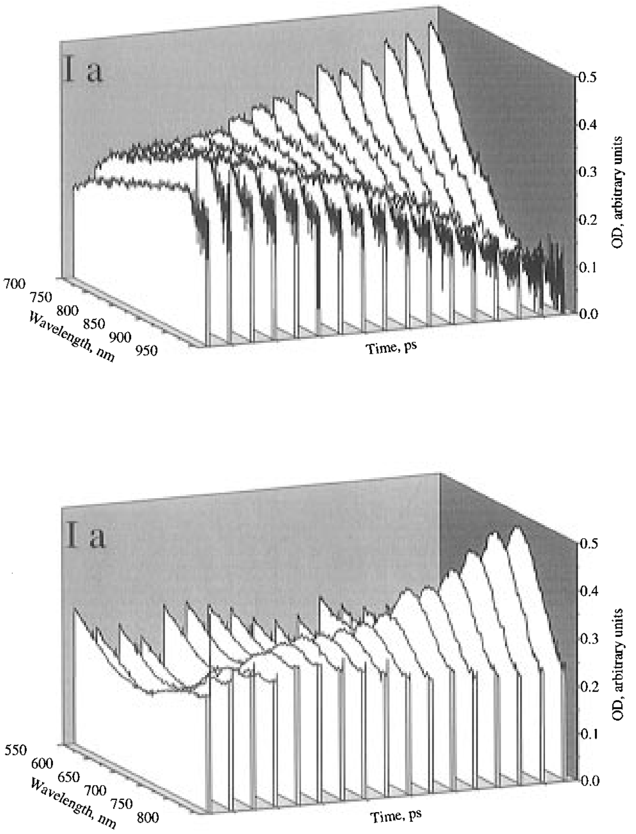

Figure 2. Transient absorbance changes observed following picosecond flash photolysis at 532 nm of the monoadduct (**Ia**) in deaerated toluene solution. Time scale: 50, 100, 150, 200, 250, 300, 400, 500, 600, 800, 1000, 1250, 1500, 2000, 3000, 4000, and 5000 ps.

pathways for the presently investigated derivatives (**I**−**III**). Laser-induced excitation of the fullerene moiety primarily leads to the formation of the excited singlet state, which usually undergoes rapid and quantitative intersystem crossing to the excited triplet state. Excitation of an electron from a low-energy bonding orbital to a high-energy antibonding orbital is known to increase the electron affinity and thus to reduce the ionization potential of the fullerene.[19] Consequently, $^3C_{60}$ or $(^3C_{60})-R$ are stronger oxidants and reductants, both subject to reaction with suitable reductive (diazabicyclooctane, DABCO)[20] and oxidative (tetracyanoquinodimethane, TCNQ) quenchers.[21] Reductive quenching of the excited triplet state involves electron transfer to the C_{60} core, and hence, it is conceivable that this leads to the formation of charge-separated ion radical pairs, e.g., $(C_{60}{}^{\bullet -})-R$ and the oxidized form of the applied quencher.

Time-Resolved Techniques. *Excited Singlet States*. To probe the singlet and excited triplet state behavior of functionalized C_{60} derivatives, time-resolved differential absorption spectra were recorded immediately following laser-induced excitation. The pump wavelength was 532 nm. Transient absorption spectra of the bis(ethoxycarbonyl)methylene monoadduct (**Ia**) (2.0×10^{-5} M) in oxygen-free toluene solution, obtained at various times, are shown in Figure 2 (upper box). The region between 700 and 960 nm reveals the formation of an absorption maximum around 920 nm that is completed around 100 ps after excitation. This resembles the general observation for pristine C_{60} in toluene.[22] This transient absorption is accordingly attributed to the excited singlet state. Its decay follows clean first-order kinetics and results in the formation of a sharp absorption around 720 nm, as shown in Figure 2 (lower box). Since the growth at 720 nm exactly parallels the decay of singlet absorption, this band is assigned to the triplet absorption. The associated singlet−triplet conversion in photoexcited **Ia** occurs with a half-life of 1.54 ns. This value is slightly higher compared to the intersystem crossing in excited pristine C_{60}.[22a]

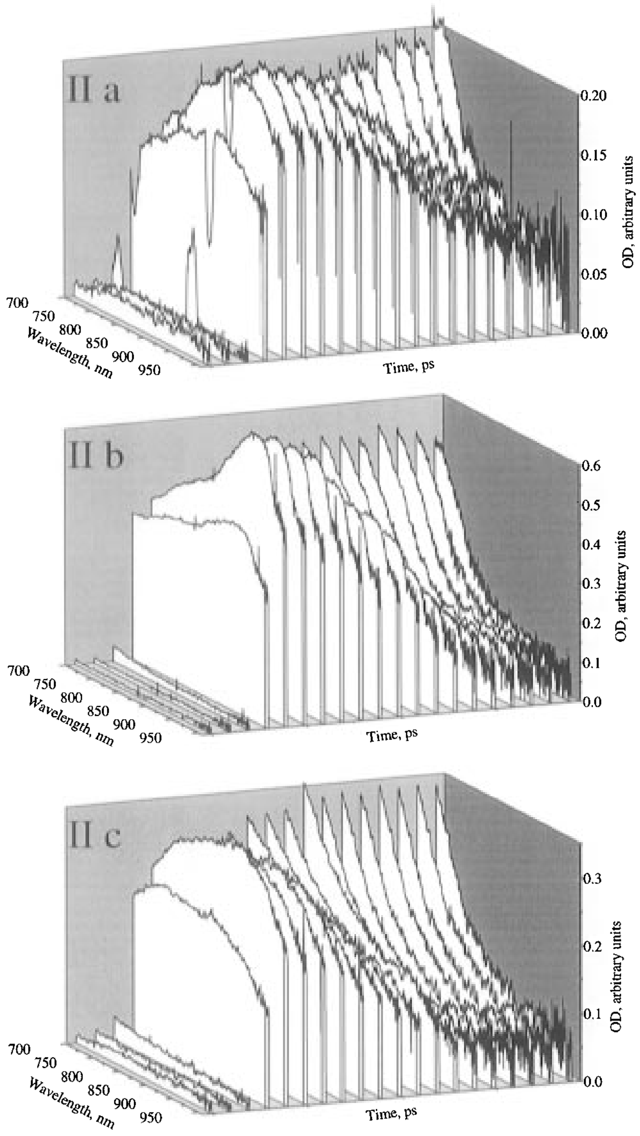

Figure 3. Transient absorbance changes observed following picosecond flash photolysis at 532 nm of bis-adducts (**IIa**, **IIb**, **and IIc**) in deaerated toluene solution. Time scale: 50, 0, 50, 100, 200, 300, 400, 500, 750, 1000, 1250, 2000, 2500, 3000, 3500, 4000, 4500, 5000, and 6000 ps.

Transient absorption spectra of derivatives **IIa**, **IIb**, and **IIc** are summarized in Figure 3. The differential absorption changes recorded around 100−200 ps after the laser pulse are, in analogy to **Ia**, ascribed to the formation of the excited singlet states of the three different bis-functionalized fullerene derivatives (note that the absorption scale of **IIa** differs strongly from **IIb** and **IIc**). However, a remarkable blue shift of the singlet−singlet ($S^*_1 \rightarrow S^*_n$) transition, ranging from 920 nm (C_{60}) to 868 nm (*e*,*e*,*e*-$C_{60}[C(COOEt)_2]_3$, **III**) was observed (Table 1). In accordance with an earlier report on triplet−triplet ($T^*_1 \rightarrow T^*_n$) absorptions,[12b] this can be rationalized in terms of a gradual perturbation of the fullerene's π-system with increasing number of functionalizing groups. The lifetime of the excited singlet state, monitored at the singlet−singlet ($S^*_1 \rightarrow S^*_n$) transition, also was significantly affected by the degree of functionalization, i.e. $\tau_{1/2}\{C_{60}[C(COOEt)_2]$ (**Ia**)$\} = 1.54$ ns; $\tau_{1/2}\{$*e*,*e*,*e*-C_{60}-$[C(COOEt)_2]_3$ (**III**)$\} = 3.12$ ns (Figure 4 for **Ia**, **IIa**, and **III**; Table 1).

TABLE 1: Photophysical Data for the Excitation of Functionalized Fullerene Derivatives and Rates for the ISC (Conversion of the Singlet Excited State into Triplet Excited State) in Toluene at RT

compound	triplet absorption [nm]	singlet absorption [nm]	singlet decay [ns]
C_{60}	747[a]	920	1.2[b]
Ia; $C_{60}[C(COOEt)_2]$	720[a]	920	1.54
Ib; $C_{60}(C_4H_6O)$	710[a]	897	
Ic; $C_{60}(C_3H_7N)$	705[c]	886[c]	1.26[c]
IIa; *e*-$C_{60}[C(COOEt)_2]_2$	710[a]	885	2.88
IIb; *trans*-3-$C_{60}[C(COOEt)_2]_2$	705[a]	895	1.96
IIc; *trans*-2-$C_{60}[C(COOEt)_2]_2$	690[a]	875	1.68
III; *e,e,e*-$C_{60}[C(COOEt)_2]_3$	650[a]	868	3.12

[a] Taken from ref 12b. [b] Taken from ref 22a. [c] Taken from ref 9c.

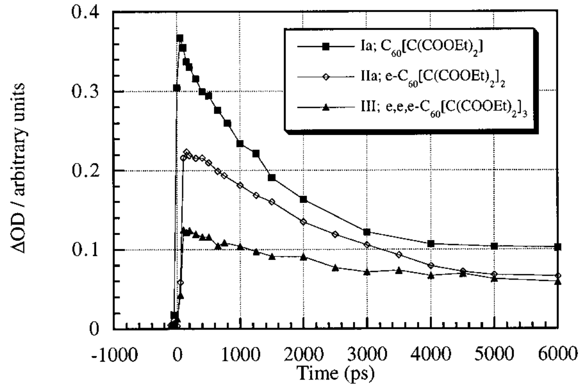

Figure 4. Time−absorption profile for **Ia**, **IIa**, and **III**, following laser excitation at 532 nm in deaerated toluene solution.

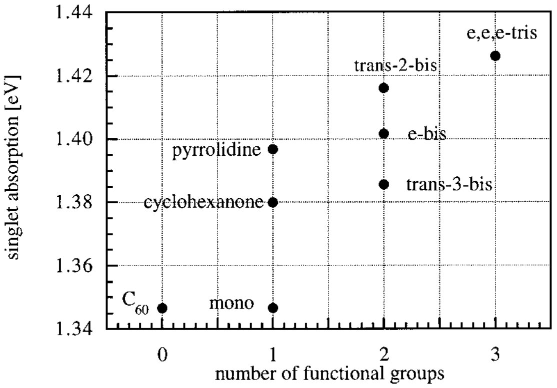

Figure 5. Plot of absorption maximum for the excited singlet energies (eV) *versus* number of bis(ethoxycarbonyl)methylene groups at the fullerene core.

It should be noted that the structural difference between the *e*-$C_{60}[C(COOEt)_2]_2$ (**IIa**) and the *e,e,e*-$C_{60}[C(COOEt)_2]_3$ derivative (**III**) comprises not only a removal of an additional C=C double bond but also an isolation of a benzenoid ring (see Figure 1), which also contributes to a modification of the chromophoric and electronic properties.

Figure 5 displays the complete correlation of the excited singlet energies *versus* the number of bis(ethoxycarbonyl)-methylene groups covalently linked to the fullerene moiety. The collected data may be interpreted as a reflection of the gradual destruction of the fullerene's π-system with an increasing number of lifted double bonds. The small blue shifts found for the cyclohexanone adduct (**Ib**) and the *N*-methylfullero-pyrrolidine derivative (**Ic**) may be attributed, at least in part, to the greater electron-withdrawing effect induced by the keto group at the cyclohexanone ring and the pyrrolidine unit, respectively, as compared to the bis(ethoxycarbonyl)methylene function in **Ia**. In addition, the size and structure of the ring fused to the fullerene core (three-membered ring for compound **Ia**, five-membered ring for derivative **Ic**, and six-membered ring for **Ib**) may affect the electronic properties of the fullerene chromophore.

In conclusion, the overall observation regarding the excited singlet energies resembles our earlier finding on the excited triplet energies.[12b] Within the series of singlet absorptions of the bis-adducts, i.e., **IIa**, **IIb**, and **IIc**, it is, however, the *trans*-3-$C_{60}[C(COOEt)_2]_2$ (**IIb**) that shows the smallest blue shift and thus seems to be the least electronically distorted isomer, compared to pristine C_{60}. This finding is in contrast to the triplet−triplet ($T^*_1 \rightarrow T^*_n$) energies, which indicated the *e*-C_{60}-$[C(COOEt)_2]_2$ (**IIa**) to be the least affected isomer.

Excited Triplet States. Generation and characterization of the triplet states of C_{60}, C_{70}, and some functionalized fullerene derivatives in nonaqueous media such as toluene or benzene have also been achieved by pulse radiolysis.[23] Radiolysis of a nitrogen-saturated toluene solution containing 0.02 M biphenyl is known to afford the formation of long-lived excited triplet states of biphenyl, namely, ^{3}BP. The low lying triplet states of **Ia** ($E_T = 1.50$ eV) and of **IIa**, **IIb**, **IIc**, and **III** (Table 2) should therefore favor an energy transfer from the high triplet energy of biphenyl ($E_T = 2.80$ eV).

This route provides an elegant method for forming excited triplet states of the functionalized fullerenes via bypassing the initial excited singlet state, thus complementing our previous flash photolytic data.[12b,c] The actual energy transfer according to eq 1 was monitored via both decay of the ^{3}BP absorption at 360 nm and the formation of the $(^3C_{60})[C(COOEt)_2]$ (**Ia**) absorption at 720 nm. This is well in line with those data obtained in earlier picosecond experiments and with some already published data.[7f,12b,c,14a] From the slopes of a linear k_{obs} *versus* fullerene concentration relationship a bimolecular rate constant of 1.8×10^{10} M^{-1} s^{-1} was derived. The corresponding values for the other functionalized fullerene derivatives were found to be diffusion controlled ($>1 \times 10^{10}$ M^{-1} s^{-1}).

$$^3\mathrm{BP} + \mathrm{C_{60}[C(COOEt)_2]}_n \xrightarrow{k_{ET}} \mathrm{BP} + (^3\mathrm{C_{60}})[\mathrm{C(COOEt)_2}]_n \quad (1)$$

The triplets generally decayed via dose-independent first-order kinetics, on a time scale of 100 μs, to regenerate the ground state.

TABLE 2: Spectroscopical Data and Reduction Potential of Ground and Excited States of Functionalized Fullerene Derivatives

compound	$^3E_{0\rightarrow 0}$ [eV]	$^1E_{0\rightarrow 0}$ [eV]	ΔE $E_{singlet} - E_{triplet}$ [eV]	Stokes shift $\Delta\nu$ [cm^{-1}]	$E_{1/2}$ ($C_{60}/C_{60}^{\bullet -}$)[a] [V] *versus* SCE	$E_{1/2}$ ($^3C_{60}/C_{60}^{\bullet -}$) [V] *versus* SCE	$E_{1/2}$ ($^1C_{60}/C_{60}^{\bullet -}$) [V] *versus* SCE
C_{60}	1.57[b]	1.99[b]	0.42		0.55	1.01	1.44
Ia; $C_{60}[C(COOEt)_2]$	1.502	1.796	0.291	20	0.64	0.86	1.16
Ib; $C_{60}(C_4H_6O)$	1.500	1.770	0.266				
Ic; $C_{60}(C_3H_7N)$	1.500	1.762	0.258	41	0.64[c]	0.86	1.12
IIa; *e*-$C_{60}[C(COOEt)_2]_2$	1.500	1.775	0.275	103	0.76	0.74	1.02
IIb; *trans*-3-$C_{60}[C(COOEt)_2]_2$	1.502	1.765	0.263	102	0.80	0.70	0.97
IIc; *trans*-2-$C_{60}[C(COOEt)_2]_2$	1.504	1.770	0.266	81	0.76	0.74	1.01
III; *e,e,e*-$C_{60}[C(COOEt)_2]_3$	1.498	1.765	0.267	164	0.86	0.64	0.91

[a] Measured in toluene, 2-propanol (9:1). [b] Taken from ref 7f. [c] Taken from ref 2b.

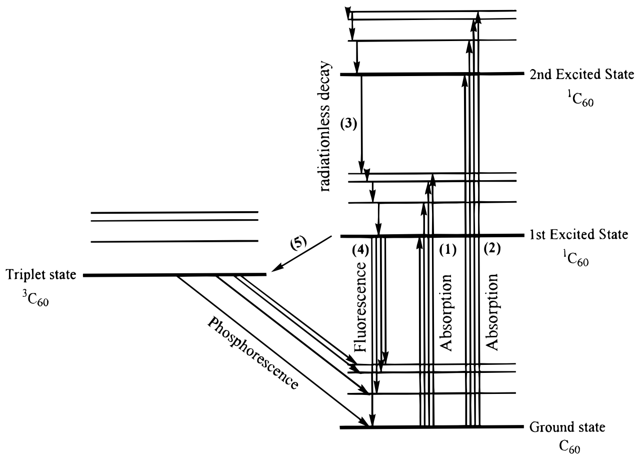

Figure 6. Schematic representation of the excitation processes of functionalized fullerene derivatives.

The triplet−triplet absorption maxima observed for **IIa** (710 nm), **IIb** (705 nm), **IIc** (690 nm), and **III** (650 nm) in these pulse radiolysis experiments essentially resemble the flash photolytic findings (Table 1). In particular, they confirm the significant blue shift of the triplet−triplet ($T^*_1 \rightarrow T^*_n$) absorption upon functionalization of the fullerene core, consisting of nearly 100 nm for *e,e,e*-($^3C_{60}$)[C(COOEt)$_2$]$_3$ (**III**) compared to pristine C_{60}.

Steady-State Techniques. The fluorescence and phosphorescence of fullerenes and their derivatives shall be discussed by reference to an energy level diagram (Figure 6). At room temperature most molecules are in the lowest vibrational level of the ground state, and light-induced transitions upward occur from here (processes 1 and 2). Transitions to particular vibrational levels might appear in the absorption spectrum as well-separated bands. After excitation to any state higher than the lowest vibrational level of the first excited state, most molecules undergo a rapid *cascade* energy degradation down to the lowest excited singlet state without light emission process 3. From this level the molecule can return to any one of the vibrational levels of the ground state by emitting fluorescence ($^10 \rightarrow 0$) (process 4). In this respect, fluorescence can be considered to be the reversed process of the singlet excitation reaction. Alternatively, photoexcited molecules may return to the ground state via intersystem crossing to the triplet state (process 5) and subsequent phosphorescence. In this case the most energetic emission refers to the ($^30 \rightarrow 0$) transition to the ground state.

Fluorescence Measurements. The fluorescence emission spectrum of C_{60}[C(COOEt)$_2$] (**Ia**), as shown in Figure 7a, has been recorded at 77 K and is a result of five scans with long integration times (20 s) and low increments (0.1 nm). It is in excellent agreement with the mirror image UV−vis absorption features, reflecting the fact that the distribution of vibrational levels in the first excited state resembles the distribution of vibrational levels in the ground state. The good match of the two respective extreme lines, i.e. the absorption band of the longest wavelength and the corresponding emission band of the shortest wavelength, and the fact that they exhibit the highest oscillator strength are a valuable aid for an unambiguous assignment of the $0 \rightarrow 0$ transition bands. Looking into detail, the respective $^*0 \rightarrow 0$ emission and $0 \rightarrow {}^*0$ absorption bands differ only very slightly, i.e. show only a small Stokes shift, as evidenced by the respective maxima at 690 and 688 nm. A similar observation has been reported earlier for **Ic**.[7f,9b] The general incoincidence of the $0 \rightarrow 0$ transitions can be ascribed to an adjustment of the fullerene's excited singlet state to the solvent environment without any significant energetic demand even though the excited state is of larger size compared to its ground state. The minor Stokes shift, or Franck−Condon instability energy, of 20 cm^{-1} is well in line with expectation for a highly symmetric sphere as in fullerenes.

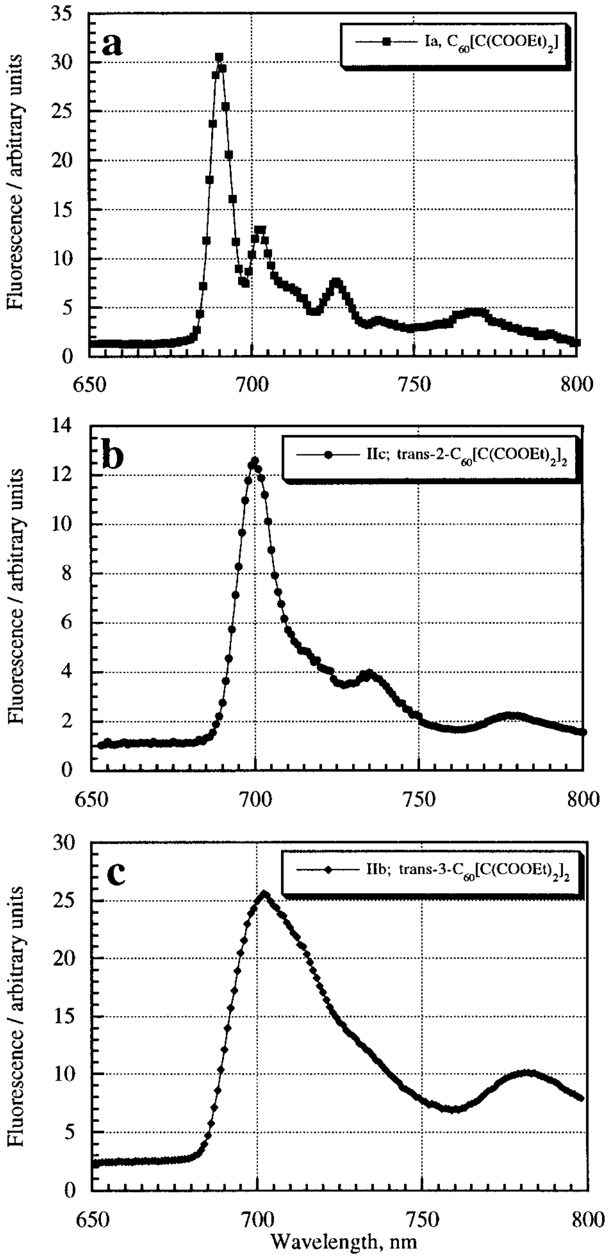

Figure 7. Fluorescence emission of 1.0 × 10^{-4} M (a) **Ia** (upper box), (b) **IIb** (center box), and (c) **IIc** (lower box) in methylcyclohexane at 77 K; excitation wavelength 337 nm.

The fluorescence spectrum of **Ia** remained basically the same upon variation of the excitation wavelength, e.g., 308, 337, and 532 nm, except for the relative intensity. Since fluorescence is always emitted from the lowest vibrational level of the first excited state, regardless to what level the electrons of the functionalized fullerene were originally raised, the location of the individual emission-related bands should, indeed, remain unaffected. The fluorescence intensity is known to depend on the molar extinction coefficient of the ground states and should consequently result in a change of the relative emission yields, i.e. intensities. C_{60} and the presently investigated fullerene derivatives do, in fact, display different molar extinction coefficients at these wavelengths.

TABLE 3: Fluorescence and Phosphorescence Emission of Functionalized Fullerene Derivatives in MeCy at 77 K

compound	fluorescence peaks [nm]	phosphorescence peak [nm]
Ia; $C_{60}[C(COOEt)_2]$	690, 703, 712 (sh), 727, 741, 771, 780 (sh)	825
Ib; $C_{60}(C_4H_6O)$	700, 716, 724 (sh), 738, 755, 784, 796 (sh)	826
Ic; $C_{60}(C_3H_7N)$	703, 716, 725 (sh), 739, 754, 783, 796 (sh)	826
IIa; *e*-$C_{60}[C(COOEt)_2]_2$	694, 678, 657, 634, 620	826
IIb; *trans*-3-$C_{60}[C(COOEt)_2]_2$	697, 684, 679, 630	825
IIc; *trans*-2-$C_{60}[C(COOEt)_2]_2$	696, 685, 677, 660, 628	824
III; *e*,*e*,*e*-$C_{60}[C(COOEt)_2]_3$	694, 672, 656, 634	827

TABLE 4: Spectral Characteristics of Functionalized Fullerene Derivatives; Fluorescence in MeCy at 77 K, Absorbance in Toluene at RT

1a; $C_{60}[C(COOEt)_2]$	absorbance [nm]	689, 679, 670, 656, 644, 626
	[cm^{-1}]	14513, 14728, 14925, 15244, 15527, 15974
	fluorescence [nm]	690, 703, 712, 727, 741, 771
	[cm^{-1}]	14493, 14224, 14045, 13755, 13492, 12970
IIa; *e*-$C_{60}[C(COOEt)_2]_2$	absorbance [nm]	694, 678, 657, 634, 620
	[cm^{-1}]	14409, 14749, 15221, 15773, 16129
	fluorescence [nm]	699, 713, 738, 757, 768, 790
	[cm^{-1}]	14306, 14025, 13550, 13210, 13021, 12658
IIb; *trans*-3-$C_{60}[C(COOEt)_2]_2$	absorbance [nm]	697, 684, 679, 630
	[cm^{-1}]	14347, 14619, 14925, 15873
	fluorescence [nm]	702, 712, 728, 782
	[cm^{-1}]	14245, 14045, 13736, 12787
IIc; *trans*-2-$C_{60}[C(COOEt)_2]_2$	absorbance [nm]	696, 685, 677, 660, 628
	[cm^{-1}]	14367, 14598, 14771, 15151, 15924
	fluorescence [nm]	700, 715, 722, 736, 778
	[cm^{-1}]	14286, 14045, 13850, 13587, 12853
III; *e*,*e*,*e*-$C_{60}[C(COOEt)_2]_3$	absorbance [nm]	694, 672, 656, 634
	[cm^{-1}]	14409, 14881, 15243, 15772
	fluorescence [nm]	702, 725, 742, 770
	[cm^{-1}]	14245, 13793, 13477, 12987

Substitution of methylcyclohexane as a solvent by dichloromethane or benzene resulted (i) in a broadening of the emission spectra, (ii) in a noticeable red shift of the $^*0 \rightarrow 0$ transition bands, and (iii) in a significant loss of resolution.

Under identical scanning conditions, the fluorescence emission spectra of the monoadducts **Ib** and **Ic** exhibited structural patterns similar to **Ia** (Table 3). The $^*0 \rightarrow 0$, $^*0 \rightarrow 1$, $^*0 \rightarrow 2$, etc., transition bands, however, were red-shifted by 10 nm for the cyclohexanone adduct (**Ib**) and 13 nm for the *N*-methylfulleropyrrolidine derivative (**Ic**). These shifts are considered to reflect the greater electron-withdrawing effect induced by the functional groups and different size of the rings fused to the fullerene cores in these derivatives as compared to the bis(ethoxycarbonyl)methylene group. This corroborates the shifts established for the excited singlet (see above) and excited triplet energies.

Data concerning the spectral characteristics of the fluorescence emission of the investigated monofunctionalized fullerene derivatives are summarized in Table 3. In general, monofunctionalization of fullerenes leads to a reasonable resolution of the emission spectra and, furthermore, to a significant enhancement of the fluorescence intensity relative to pristine C_{60}. This can be ascribed, at least in part, to a change of symmetry from I_h (C_{60}) to C_{2v} (monoadducts). The enhanced fluorescence in these compounds has recently been ascribed to a decrease in the rate of the intersystem crossing (ISC) between the first excited singlet and triplet states, induced by the partially broken π-system.[12d] Our results do not support this conclusion since in the monofunctionalized compounds the observed rate for the intersystem crossing resembles that for pristine C_{60}.

The situation is quite different upon addition of a second bis(ethoxycarbonyl)methylene group to the fullerene core, as can be depicted from the emission spectra of **IIb** and **IIc** displayed in Figure 7b,c. Changing the symmetry of the functionalized fullerene derivative from C_{2v} (**Ia**) to C_2 (**IIb** and **IIc**) resulted (i) in a red shift of the main emission ($^*0 \rightarrow 0$) band, (ii) in a remarkable broadening of the emission band, and (iii) in a significant loss of resolution. The absorption spectra of **IIb** and **IIc**, which, incidentally, were found to be mirror images of the emission spectra, confirmed this trend impressively. The same basically holds for the other multiply-functionalized fullerenes, although the picture may be even more complicated, as can be seen in the fluorescence spectra of derivatives **IIa** (C_s) and **III** (C_3). For example, the emission spectrum of the *e*-$C_{60}[C(COOEt)_2]_2$ (**IIa**) isomer showed a low-intensity hot band around 685 nm. Furthermore, two transition bands of strong oscillator strength (similar to the $^*0 \rightarrow 0$ transition band) were monitored at 715 and 757 nm. There is no doubt that these spectra originated from the emission of **IIa** and **III** since their excitation spectra show similarities in spectral structure to the corresponding absorption spectra.

For further quantitative discussion, the conventional wavelength-dependent emission and absorption spectra were converted into wavenumber plots. This aids in the identification and correlation of the fine structure between absorption and emission features. To rule out any false assignment, the wavenumber (see Table 4) and wavenumber differences ($\Delta\nu$) between the assigned $0 \rightarrow 0$ bands and the preceding absorption or following emission bands were calculated. The sets of $\Delta\nu$ are seen to be in reasonably good agreement with each other and, thus, corroborate the validity of the $0 \rightarrow 0$ assignments. For instance, by ascribing the 694-nm (14 409-cm^{-1}) absorption of **III** to the $0 \rightarrow {}^*0$ transition, the wavenumber differences ($\Delta\nu$) for the three preceding absorption features are 472, 834, and 1363 cm^{-1}, in fairly good agreement with the $\Delta\nu$ (452, 768, 1258 cm^{-1}) relative to the emission peak at 702 nm (14 245 cm^{-1}). Assignment of the $^*0 \rightarrow 0$ transition to a different emission band would result in a complete mismatch of the $\Delta\nu$'s with those derived from the absorption spectrum.

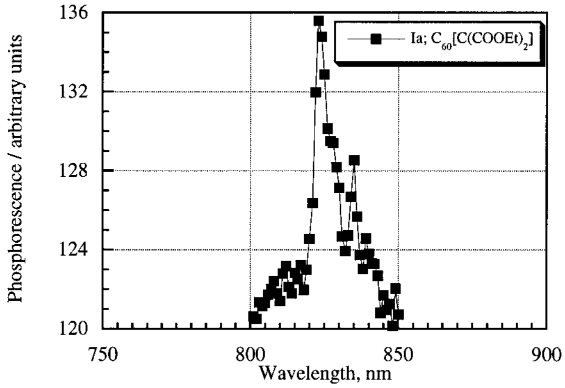

Figure 8. Phosphorescence-related emission of **Ia** (1.0×10^{-4} M) in methylcyclohexane, 2-methyltetrahydrofuran, ethyl iodide (2:1:1 v/v) at 77 K; excitation wavelength 337 nm.

The assigned *0 → 0 transition bands of the various derivatives are listed in Table 4. In line with the absorption spectra of the excited singlet states, the observed fluorescence data can be rationalized in terms of a gradual perturbation of the fullerene's π-system with increasing number of functionalized C=C bonds. It is interesting to note that among the studied bis-adducts, namely, **IIa**, **IIb**, and **IIc**, the *e*-$C_{60}[C(COOEt)_2]_2$ (**IIa**) isomer exhibits the least distortion, compared to pristine C_{60}. In contrast to the expectation, the location of the *0 → 0 transition of **III** was nearly unchanged relative to **IIb**. We cannot offer any rationale for this at the moment.

Phosphorescence Measurements. The excited singlet state of fullerenes is efficiently converted to the excited triplet state by rapid and quantitative intersystem crossing, ISC (see process 5 in Figure 6). However, as we demonstrated above, an increasing number of addends (bis(ethoxycarbonyl)methylene groups) attached to the fullerene core enhances the lifetime of the excited singlet state and consequently decelerates the ISC process. External heavy atom effect, on the other hand, is known to accelerate the transformation rate from the excited singlet to the excited triplet state.[15a,22c] Fullerene-related emissions of **Ia** were completely abolished, for example, in a solvent mixture consisting of methylcyclohexane, 2-methyltetrahydrofuran, and ethyl iodide as heavy atom provider (2:1:1 v/v). Instead, a new but weak band appeared at 825 nm, as shown in Figure 8, attributable to phosphorescence. This finding implies a significant red shift of the phosphorescence-related emission relative to pristine C_{60} and resembles the observations described in some earlier studies.[7f,9b] The low intensity, i.e. low transition probability, is explained by the fact that radiative transitions between states of different multiplicity are principally forbidden. Alternatively to the external heavy atom experiment, phosphorescence measurements were also carried out in neat methylcyclohexane by employing a short time delay between the excitation and detection.

The peaks of the phosphorescence bands of the monoadducts **Ib** and **Ic** nearly coincide with **Ia**, displaying just a minor red shift of around 1 nm. The current observation demonstrates that functionalization with groups that impose different electron-withdrawing forces on the fullerene's π-system leads only to minor changes of the triplet energies of the respective monofunctionalized fullerene derivatives.

The phosphorescence spectra of derivatives **IIa**, **IIb**, and **IIc** also exhibited practically no spectral shifts. Only for the tris-functionalized derivative **III** was a small one, by 2 nm (to 827 nm), observed. The respective data are listed in Table 3.

The current observation demonstrates that functionalization of the fullerene core imposes only minor effects on the triplet energies of the respective functionalized fullerene derivatives (*0 → 0 transition). This is remarkable, since significant changes have been monitored for the singlet−singlet ($S^*_1 \rightarrow S^*_n$) and triplet−triplet ($T^*_1 \rightarrow T^*_n$) and some changes for the fluorescence-related *0 → 0 transitions.

Among the three isomeric bis-adducts, e.g., **IIa**, **IIb**, and **IIc**, the resonance within the π-system of both the *e*-$C_{60}[C(COOEt)_2]_2$ isomer (**IIa**) and the *trans*-2-$C_{60}[C(COOEt)_2]_2$ isomer (**IIc**) seemed equally least affected by the degree of functionalization. This finding is somehow in contrast to the triplet−triplet ($T^*_1 \rightarrow T^*_n$) and the fluorescence-related *0 → 0 energies, where it is the *e*-$C_{60}[C(COOEt)_2]_2$ (**IIa**) alone that exhibits the highest resonance stability.

Comparison of Optical Data. Summarizing the optical data, our present findings confirm earlier data and the conclusion that perturbation of the fullerene's π-system via lifting of double bonds through functionalization results in higher energies required for singlet−singlet ($S^*_1 \rightarrow S^*_n$) and triplet−triplet ($T^*_1 \rightarrow T^*_n$) transitions (blue-shifted absorptions) as compared to pristine C_{60}. The energy difference between the ground state and the first excited triplet and singlet state, as they emerge from the phosphorescence and fluorescence measurements, on the other hand, decreases upon functionalization. This would reflect a particularly high degree of resonance stabilization of C_{60} as compared to the functionalized molecules in the ground state. Further promotion beyond the first excited states requires considerably lower energies within the singlet than in the triplet term. As a result, the S^*_2 level for C_{60} lies only slightly above the T^*_2 level (3.33 *versus* 3.22 eV over S_0), while in case of *e*,*e*,*e*-$C_{60}[C(COOEt)_2]_3$ (**III**) the situation has already become reverse, with T^*_2 (3.39 eV) located above S^*_2 (3.19 eV). Furthermore, the structure of the *e*,*e*,*e*-$C_{60}[C(COOEt)_2]_3$ derivative (**III**) reveals isolation of a benzenoid ring (see Figure 1), which also might account for these modified electronic properties. The S_1-T_1 energy differences finally are almost the same for all functionalized systems (0.26−0.29 eV), and only for pristine C_{60} has a significantly higher value (0.42 eV) been measured. This may explain why the rate constant for intersystem crossing does not exhibit any trend within the series of the functionalized fullerenes. But the reported lifetime for pristine C_{60} ($\tau_{1/2}$ = 1.2 ns) is also of the same order of magnitude. A direct correlation may, in fact, not be warranted due to possible self-quenching, i.e. dependence of the lifetime on the fullerene concentration.

Cyclic Voltammetry Measurements. Electrochemical cyclic voltammetry measurements on the redox potential of the first reduction step have been performed with **Ia**, **IIa**, and **III** in a preliminary work of ours.[12b,c] In the present investigation this work was extended to determine the respective values for the electrochemical-induced reduction of **IIb** and **IIc** in toluene. Employing a sufficient concentration of a supporting electrolyte (0.1 M $Bu_4N^+BF_4^-$), however, required its initial dissolution in 10 vol % 2-propanol with subsequent addition to the toluene solution containing the functionalized fullerene derivative. The measured potentials of −0.76 and −0.80 V *versus* SCE for **IIb** and **IIc**, respectively, are reasonably in line with the reduction potential found for the *e*-$C_{60}[C(COOEt)_2]_2$ isomer (**IIa**) (−0.76 V *versus* SCE). Similarly, the degree of reversibility for the underlying reduction derived from (i) the peak separation between reduction and reoxidation ($E_{ox} - E_{red}$; **IIb** = 70 mV, **IIc** = 62 mV) and (ii) the ratio between cathodic and anodic current (i_{ox}/i_{red}; **IIb** = 0.29, **IIc** = 0.28) was found to be much lower than in the case of C_{60} and **Ia**.[12b] Although these measurements were performed in a solvent of a low dielectric constant which, due to IR drop difficulties, frequently leads to a larger peak separation than in higher dielectric media, the general conclusion of a more difficult reduction in anhydrous 1,2-dichloroethane containing 0.1 M $Bu_4N^+BF_4^-$ has been confirmed by analogous measurements of **Ia**−**III**.

Thermodynamic Correlation. In a recent report regarding the reductive quenching of derivatives **Ia**−**III** with diazabicyclooctane (DABCO), we found that functionalization of C_{60} leads to a tremendous deceleration of the quenching process by more than 3 orders of magnitude ($k_q(\mathbf{III}) = 1.3 \times 10^6$ M^{-1} s^{-1}) relative to C_{60} ($k_q(C_{60}) = 2.5 \times 10^9$ M^{-1} s^{-1}).[12b,c] In the following a correlation will be established that links these kinetic data with the electrochemical and optical parameters measured in the present study. For such a quantitative evaluation it has be kept in mind that the standard electrochemical CV experiments provide the redox potential for the ground state C_{60} or C_{60}−R, while the reductive quenching rates refer to the corresponding excited triplet entities, $^3C_{60}$ and $(^3C_{60})$−R.

The entire thermodynamics of excited states has been extensively discussed in earlier studies.[24] Here we will focus on the evaluation of the difference between the redox potentials of $C_{60}[C(COOEt)_2]_n/(C_{60}^{\bullet -})[C(COOEt)_2]_n$ and $(^*C_{60})[C(COOEt)_2]_n/(C_{60}^{\bullet -})[C(COOEt)_2]_n$ couples, where $C_{60}[C(COOEt)_2]_n$ is the ground state fullerene, $(^*C_{60})[C(COOEt)_2]_n$ represents any excited state, e.g., singlet or triplet, and n indicates the number of addends ($n = 1, 2, 3$).

Excitation of an electron from a low-energy bonding orbital to a high-energy antibonding orbital is known to result in an increase of the electron affinity and a decrease in the fullerene's ionization potential. Thus, electronically excited C_{60} becomes a moderately strong oxidant and at the same time a strong reductant. The electrochemical redox potentials of the couples $C_{60}/(C_{60}^{\bullet -})$, $(^1C_{60})/(C_{60}^{\bullet -})$, and $(^3C_{60})/(C_{60}^{\bullet -})$ and the respective functionalized fullerene derivatives **Ia**−**III** *versus* a reference couple (D/D$^+$) can be discussed in terms of the free energy changes in eqs 2 and 3.

$$C_{60} + D \rightarrow (C_{60}^{\bullet -}) + D^+ \tag{2}$$

$$(^3C_{60}) + D \rightarrow (C_{60}^{\bullet -}) + D^+ \tag{3}$$

The difference in the free energy changes of reactions 2 and 3 can be expressed as follows:

$$\begin{aligned}\Delta G[C_{60}/(C_{60}^{\bullet -})] - \Delta G[(^3C_{60})/(C_{60}^{\bullet -})] &= \\ \Delta H[C_{60}/(C_{60}^{\bullet -})] - \Delta H[(^3C_{60})/(C_{60}^{\bullet -})] &- \\ T\{\Delta S[C_{60}/(C_{60}^{\bullet -})] - \Delta S[(^3C_{60})/(C_{60}^{\bullet -})]\}&\end{aligned} \tag{4}$$

It is well-known that changes with respect to the shape, size, and solvation between excited states and ground states cause a Stokes shift between absorption and emission. The small Stokes shifts for C_{60} and functionalized fullerenes, as summarized in Table 2, indicate that these changes are almost negligible, suggesting correspondingly negligible entropy differences between the ground and excited states, i.e.

$$T\Delta S \approx 0 \tag{5}$$

and

$$\Delta(\Delta G) \approx \Delta(\Delta H) \tag{6}$$

Assuming a constant volume for the individual redox processes and no Coulombic work terms, eq 6 can thus be formulated as

$$\Delta G = -nF\Delta E \tag{7}$$

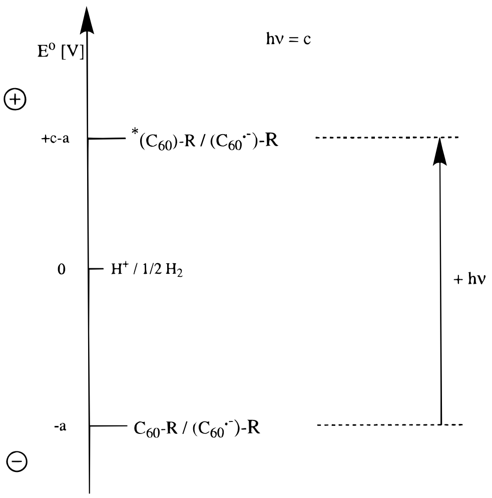

Figure 9. Schematic diagram showing the difference in the redox properties of the ground state C_{60} $\{E°[C_{60}/(C_{60}^{\bullet -})]\}$ and excited $^1C_{60}$ and $^3C_{60}$ $\{E°[(^*C_{60})/(C_{60}^{\bullet -})]\}$. c is the one-electron potential corresponding to the zero−zero spectroscopic energy of the excited state $\{E_{0\rightarrow 0}[C_{60} \rightarrow (^*C_{60})]\}$.

where F is the Faraday constant. Hence, for excited states of C_{60} the reduction potentials $E°\{(^3C_{60})[C(COOEt)_2]_n/(C_{60}^{\bullet -})[C(COOEt)_2]_n\}$ are approximately given by the reduction potentials of the ground state ($E°\{C_{60}[C(COOEt)_2]_n/(C_{60}^{\bullet -})[C(COOEt)_2]_n\}$) plus an energy term corresponding to the zero−zero spectroscopic energy of the excited state ($E_{0\rightarrow 0}\{C_{60}[C(COOEt)_2]_n \rightarrow (^3C_{60})[C(COOEt)_2]_n\}$). This leads to eq 8 (for an illustration see Figure 9, where c represents the one-electron potential corresponding to the zero−zero spectroscopic energy). The $E_{0\rightarrow 0}[C_{60} \rightarrow (^*C_{60})]$ term is, of course, numerically identical with the energy of the highest energy phosphorescence band, allowing an easy determination of the relevant reduction potential of the excited triplet state. The same kind of calculation can, of course, be made for the singlet state. The corresponding data are listed in Table 2.

$$E°[(^3C_{60})/(C_{60}^{\bullet -})] = E°[C_{60}/(C_{60}^{\bullet -})] + E_{0\rightarrow 0}[C_{60} \rightarrow (^3C_{60})] \tag{8}$$

The emission studies revealed that functionalization of C_{60} leads only to minor, if any, changes for $E_{0\rightarrow 0}$. The respective $E°[(^1C_{60})/(C_{60}^{\bullet -})]$ and $E°[(^3C_{60})/(C_{60}^{\bullet -})]$ thus appear to correlate linearly to the redox potential of the ground state, $E°[C_{60}/(C_{60}^{\bullet -})]$. On this level, it is evident that functionalization of pristine C_{60} obstructs the ease of the underlying reduction process in both the ground and the excited state. An increasing number of bis(ethoxycarbonyl)methylene groups shift the redox potential of $^3C_{60}$ from 1.01 to 0.64 V for the *e*,*e*,*e*-$(^3C_{60})[C(COOEt)_2]_3$ (**III**). Similarly, the corresponding singlet states are shifted from 1.44 to 0.91 V (all *versus* SCE).

A semilogarithmic plot of ln $k_{\text{quenching}}$ for the reductive triplet quenching *versus* $E°[(^3C_{60})/(C_{60}^{\bullet -})]$ is shown in Figure 10. It reveals a fairly linear correlation over the entire range of rate constants covered. A limiting value, as to be expected for a purely diffusion-controlled process, has not been reached yet with our compounds.

Conclusion

In summary, time-resolved and steady-state studies, by means of radical- and light-induced techniques, have revealed most informative details on the influence of different functionalizing groups at the fullerene core on the photophysical properties of

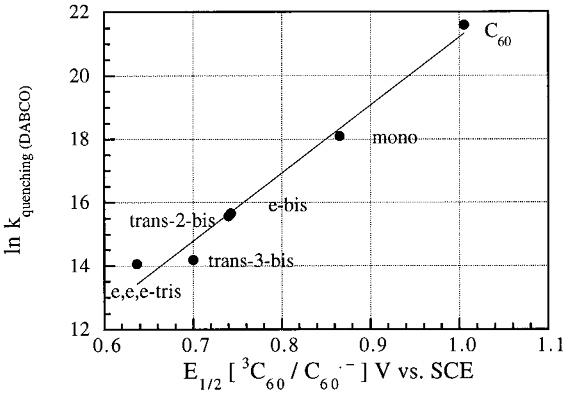

Figure 10. Semilogarithmic plot of ln $k_{\mathrm{quenching}}$ with diazabicyclooctane (DABCO) *versus* the redox potential of the first reduction step of the excited triplet state $E°[(^3C_{60})/(C_{60}^{\bullet-})]$.

functionalized C_{60}. The site and degree of functionalization sensitively impacts the physicochemical parameters of these fullerene derivatives and can be rationalized in terms of perturbation of the fullerene's π-system. Thus, the photophysical properties of functionalized C_{60} may serve as convenient markers for their analytical identification.

A correlation linking the reductive quenching rates of excited triplet fullerenes with electrochemically determined redox potentials and optical parameters shows that functionalization of pristine C_{60} obstructs the ease of reduction in both the ground and the excited state. The optical and redox properties were most significantly affected upon lifting the first C=C double bond. Higher degrees of functionalization show lesser effects. Monofunctionalization is known to result in a significant loss in the heat of formations (ΔH_f) relative to pristine C_{60} by introduction of a sp^3-hybridized carbon, locally reducing the fullerene's curvature. Subsequent bis- and tris-functionalization thus exerts only a minor further impact on perturbation of the fullerene's π-system. It is interesting to note that among the various bis-adducts the e-$C_{60}[C(COOEt)_2]_2$ (**IIa**) isomer exhibits the least distortion, compared to pristine C_{60}.

Acknowledgment. This work was supported by the Office of Basic Energy Sciences of the U.S. Dept. of Energy. This is contribution No. NDRL-3971 from the Notre Dame Radiation Laboratory.

References and Notes

(1) (a) Taylor, R.; Walton, D. R. M. *Nature* **1993**, *363*, 685. (b) Hirsch, A. *The Chemistry of the Fullerenes*; Thieme: Stuttgart, New York, 1994. (c) Diederich, F.; Thilgen, C. *Science* **1996**, *271*, 317.

(2) (a) Wilson, S. R.; Kaprindis, N.; Wu, Y.; Schuster, D. I. *J. Am. Chem. Soc.* **1993**, *115*, 8495. (b) Maggini, M.; Scorrano, G.; Prato, M. *J. Am. Chem. Soc.* **1993**, *115*, 9798. (c) Belik, P.; Gügel, A.; Spickerman, J.; Müllen, K. *Angew. Chem., Int. Ed. Engl.* **1993**, *32*, 78. (d) Zhang, X.; Foote, C. *J. Am. Chem. Soc.* **1995**, *117*, 4271. (e) Prato, M.; Maggini, M.; Giacometti, C.; Scorrano, G.; Sandoma, G.; Farnia, G. *Tetrahedron* **1996**, *52*, 5221.

(3) (a) Bausch, J. W.; Prakash, G. K. S.; Olah, G. A.; Tse, D. S.; Lorents, D. C.; Bae, Y. K.; Malhotra, R. *J. Am. Chem. Soc.* **1991**, *113*, 3205. (b) Caron, C.; Subramanian, R.; D'Souza, F.; Kim, J.; Kutner, W.; Jones, M. T.; Kadish, K. M. *J. Am. Chem. Soc.* **1993**, *115*, 8505.

(4) (a) Bingel, C. *Chem. Ber.* **1993**, *126*, 1957. (b) Hirsch, A.; Lamparth, I.; Karfunkel, H. R. *Angew. Chem., Int. Ed. Engl.* **1994**, *33*, 437. (c) Bingel, C.; Schiffer, H. *Liebigs Ann. Chem.* **1995**, 1551. (d) Lamparth, I.; Maichle-Mössmer, C.; Hirsch, A. *Angew. Chem., Int. Ed. Engl.* **1995**, *34*, 1607. (e) Schick, G.; Hirsch, A.; Mauser, H.; Clark, T. *Chem. Eur. J.* **1996**, *2*, 935.

(5) (a) Flagan, P. J.; Calabrese, J. C.; Malone, B. *Science* **1991**, *252*, 1160. (b) Lerke, S. A.; Evans, D. H.; Flagan, P. J. *J. Electroanal. Chem.* **1995**, *383*, 127. (c) Schreiner, S.; Gallaher, T. N.; Parsons, H. K. *Inorg. Chem.* **1994**, *33*, 3021.

(6) (a) Tutt, L. W.; Kost, A. *Nature* **1992**, *356*, 225. (b) Sun, R.; Li, Y.; Zheng, J.; Li, D.; Fan, Y.; Zhang, X. *Thin Solid Films* **1994**, *248*, 100. (c) Mirkin, C. A.; Caldwell, W. B. *Tetrahedron* **1996**, *52*, 5113.

(7) (a) Khan, S. I.; Oliver, A. M.; Paddon-Row, M. N.; Rubin, Y. *J. Am. Chem. Soc.* **1993**, *115*, 4919. (b) Rasinkangas, M.; Pakkanen, T. T.; Pakkanen, T. A. *J. Organomet. Chem.* **1994**, *476*, C6. (c) Liddell, P. A.; Sumida, J. P.; Mac Pherson, A. N.; Noss, L.; Seely, G. R.; Clark, K. N.; Moore, A. L.; Moore, T. A.; Gust, D. *Photochem. Photobiol.* **1994**, *60*, 537. (d) Linssen, T. G.; Dürr, K.; Hanack, M.; Hirsch, A. *J. Chem. Soc., Chem. Commun.* **1995**, 103. (e) Diederich, F.; Dietrich-Buchecker, C.; Nierengarten, J.-F.; Sauvage, J.-P. *J. Chem. Soc., Chem. Commun.* **1995**, 781. (f) Williams, R. M.; Zwier, J. M.; Verhoeven, J. W. *J. Am. Chem. Soc.* **1995**, *117*, 4093. (g) Imahori, H.; Hagiwara, K.; Akiyama, T.; Taniguchi, S.; Okada, T.; Sakata, Y. *Chem. Lett.* **1995**, 265. (h) Maggini, M.; Dono, A.; Scorrano, G.; Prato, M. *J. Chem. Soc., Chem. Commun.* **1995**, 845. (i) Anderson, J. L.; An, Y.-Z.; Rubin, Y.; Foote, C. S. *J. Am. Chem. Soc.* **1994**, *116*, 9763. (j) Nakamura, Y.; Minowa, T.; Hayashida, Y.; Tobita, S.; Shizuka, H.; Nishimura, J. *J. Chem. Soc., Faraday Trans.* **1996**, *92*, 377. (k) Armspach, D.; Constable, E. C.; Diederich, F.; Housecroft, C. E.; Nierengarten, J.-F. *J. Chem. Soc., Chem. Commun.* **1996**, 2009. (l) Kuciauskas, D.; Lin, S.; Seely, G. R.; Moore, A. L.; Moore, T. A.; Gust, D.; Drovetskaya, T.; Reed, C. A.; Boyd, P. D. W. *J. Phys. Chem.* **1996**, *100*, 15926.

(8) (a) Tokuyama, H.; Yamago, S.; Nakamura, E.; Shiraki, T.; Sugiura, Y. *J. Am. Chem. Soc.* **1993**, *115*, 7918. (b) An, Y. Z.; Anderson, J. L.; Rubin, Y. *J. Org. Chem.* **1993**, *58*, 4799. (c) Diederich, F.; Jonas, U.; Gramlich, V.; Herrmann, A.; Ringsdorf, H.; Thilgen, C. *Helv. Chim. Acta* **1993**, *76*, 2445. (d) Win, W. W.; Kao, M.; Eiermann, M.; McNamara, J. J.; Wudl, F.; Pole, D. L.; Kassam, K.; Warkentin, J. *J. Org. Chem.* **1994**, *59*, 5871. (e) Jonas, U.; Cardullo, F.; Belik, P.; Diederich, F.; Gügel, A.; Harth, E.; Herrmann, A.; Isaacs, L.; Müllen, K.; Ringsdorf, H.; Thilgen, C.; Uhlmann, P.; Vasella, A.; Waldraff, C. A. A.; Walter, M. *Chem. Eur. J.* **1995**, *1*, 243. (f) Matsumoto, M.; Tachibana, H.; Azumi, R.; Tanaka, M.; Nakamura, T.; Yunome, G.; Abe, M.; Yamago, S.; Nakamura, E. *Langmuir* **1995**, *11*, 660. Arias, F.; Godinez, L. A.; Wilson, S. R.; Kaifer, A. E.; Echegoyen, L. *J. Am. Chem. Soc.* **1996**, *118*, 6086.

(9) (a) Sariciftci, N. S.; Wudl, F.; Heeger, A. J.; Maggini, M.; Scorrano, G.; Prato, M.; Bourassa, J.; Ford, P. C. *Chem. Phys. Lett.* **1995**, *247*, 510. (b) Williams, R. M.; Koeberg, M.; Lawson, J. M.; An, Y.-Z.; Rubin, Y.; Paddon-Row, M. N.; Verhoeven, J. W. *J. Org. Chem.* **1996**, *61*, 5055. (c) Guldi, D. M.; Maggini, M.; Scoranno, G.; Prato, M. *J. Am. Chem. Soc.*, in press.

(10) (a) Obeng, Y. S.; Bard, A. J. *J. Am. Chem. Soc.* **1991**, *113*, 6279. (b) Maliszewskyj, N. C.; Heiney, P. A.; Jones, D. R.; Strongin, R. M.; Chichy, M. A.; Smith, A. B. *Langmuir* **1993**, *9*, 1439. (c) Nakamura, T.; Tachibana, H.; Yumura, M.; Matsumoto, M.; Azumi, R.; Tanaka, M.; Kawabata, Y. *Langmuir* **1992**, *8*, 4. (d) Hawker, C. J.; Saville, P. M.; White, J. W. *J. Org. Chem.* **1994**, *59*, 3503. (e) Vaknin, D.; Wang, J. Y.; Uphaus, R. A. *Langmuir* **1995**, *11*, 1435. (f) Maggini, M.; Karlsson, A.; Pasimeni, L.; Scorrano, G.; Prato, M.; Valli, L. *Tetrahedron Lett.* **1994**, *35*, 2985. (g) Ravaine, S.; Le Pecq, F.; Mingotaud, C.; Delhaes, P.; Hummelen, J. C.; Wudl, F.; Patterson, L. K. *J. Phys. Chem.* **1995**, *99*, 9551. (h) Guldi, D. M.; Yian, Y.; Fendler, J. H.; Hungerbühler, H.; Asmus, K.-D. *J. Phys. Chem.* **1995**, *99*, 17673.

(11) (a) Schinazi, R. F.; Sijbesma, R.; Srdanov, G.; Hill, C. L.; Wudl, F. *Antimicrob. Agents Chemother.* **1993**, *37*, 1707. (b) Sijbesma, R.; Srdanov, G.; Wudl, F.; Castoro, J. A.; Wikins, C.; Friedman, S. H.; DeCamp, D. L.; Kenyon, G. L. *J. Am. Chem. Soc.* **1993**, *115*, 6510. (c) Friedman, S. H.; DeCamp, D. L.; Sijbesma, R.; Srdanov, G.; Wudl, F. *J. Am. Chem. Soc.* **1993**, *115*, 6506.

(12) (a) Anderson, J. L.; An, Y.-Z.; Rubin, Y.; Foote, C. S. *J. Am. Chem. Soc.* **1994**, *116*, 9763. (b) Guldi, D. M.; Hungerbühler, H.; Asmus, K.-D. *J. Phys. Chem.* **1995**, *99*, 9380. (c) Guldi, D. M.; Hungerbühler, H.; Asmus, K.-D. *J. Phys. Chem.* **1995**, *99*, 13487. (d) Nakamura, Y.; Minowa, T.; Tobita, S.; Shizuka, H.; Nishimura, J. *J. Chem. Soc., Perkin Trans. 2* **1995**, 2351. (e) Bensansson, R. V.; Bienvenue, E.; Janot, J.-M.; Leach, S.; Seta, P.; Schuster, D. I.; Wilson, S. R.; Zhao, H. *Chem. Phys. Lett.* **1995**, *245*, 566. (f) Bennati, M.; Grupp, A.; Mehring, M.; Belik, P.; Gügel, A.; Müllen, K. *Chem. Phys. Lett.* **1995**, *240*, 622. (g) Brezová, V.; Stasko, A.; Rapta, P.; Domschke, G.; Bartl, A.; Dunsch, L. *J. Phys. Chem.* **1995**, *99*, 16234.

(13) (a) Subramanian, R.; Boulas, P.; Vijayashree, M. N.; D'Souza, F.; Jones, M. T.; Kadish, K. M. *J. Chem. Soc., Chem. Commun.* **1994**, 1847. (b) Suzuki, T.; Maruyama, Y.; Akasaka, T.; Ando, W.; Kobayashi, K.; Nagase, S. *J. Am. Chem. Soc.* **1994**, *116*, 1359. (c) Zhou, F.; VanBerkel, G. J.; Donovan, B. T. *J. Am. Chem. Soc.* **1994**, *116*, 5485. (d) Eiermann, M.; Haddon, R. C.; Knight, B.; Li, Q. C.; Maggini, M.; Martin, N.; Ohno, T.; Prato, M.; Suzuki, T.; Wudl, F. *Angew. Chem., Int. Ed. Engl.* **1995**, *34*, 1591. (e) Arias, F.; Echegoyen, L.; Wilson, S. R.; Lu, Q.; Lu, Q. *J. Am. Chem. Soc.* **1995**, *117*, 1422. (f) Boudon, C.; Gisselbrecht, J.-P.; Gross, M.; Isaacs, L.; Anderson, H. L.; Faust, R.; Diederich, F. *Helv. Chim. Acta* **1995**, *78*, 1334. (g) Cardullo, F.; Isaacs, L.; Diederich, F.; Gisselbrecht, J.-P.; Boudon, C.; Gross, M. *J. Chem. Soc., Chem. Commun.* **1996**, 797. (h) Liu, N.; Touhara, H.; Morio, Y.; Komichi, D.; Okino, F.; Kawasaki, S. *J. Electrochem. Soc.* **1996**, *143*, L 214.

(14) (a) Kim, D.; Lee, M.; Suh, Y. D.; Kim, S. K. *J. Am. Chem. Soc.* **1992**, *114*, 4429. (b) Williams, R. M.; Verhoeven, J. W. *Chem. Phys. Lett.* **1992**, *194*, 446. (c) Sun, Y.-P.; Wang, P.; Hamilton, N. B. *J. Am. Chem. Soc.* **1993**, *115*, 6378. (d) Catalan, J.; Elguero, J. *J. Am. Chem. Soc.* **1993**, *115*, 9249. (e) Lin, S.-K.; Shiu, L.-L.; Chien, K.-M.; Luh, T.-Y.; Lin, T.-I. *J. Phys. Chem.* **1995**, *99*, 105. (f) Zhou, D.; Tan, H.; Gan, I.; Luo, C.; Huang, C.; Yao, G.; Zhang, P. *Chem. Lett.* **1995**, 649.

(15) (a) Zeng, Y.; Biczok, L.; Linschitz, H. *J. Phys. Chem.* **1992**, *96*, 5237. (b) van den Heuvel, D. J.; Chan, I. Y.; Groenen, E. J. J.; Matsushita, M.; Schmidt, J.; Meijer, G. *Chem. Phys. Lett.* **1995**, *233*, 284. (c) van den Heuvel, D. J.; Chan, I. Y.; Groenen, E. J. J.; Schmidt, J.; Meijer, G. *Chem. Phys. Lett.* **1994**, *231*, 111.

(16) Ebbesen, T. W. *Rev. Sci. Instrum.* **1988**, *59*, 1307.

(17) Nagarajan, V.; Fessenden, R. W. *J. Phys. Chem.* **1985**, *89*, 2330.

(18) (a) Schuler, R. H. *J. Phys. Chem.*, to be published. (b) Asmus, K.-D. *Methods Enzymol.* **1984**, *105*, 167.

(19) (a) Arbogast, J. W.; Darmanyan, A. P.; Foote, C.; Rubin, Y.; Diederich, F. N.; Alvarez, M. M.; Anz, S. J.; Whetten, R. L. *J. Phys. Chem.* **1991**, *95*, 11. (b) Arbogast, J. W.; Foote, C. *J. Am. Chem. Soc.* **1991**, *113*, 8886. (c) Sension, R.; Szarka, A. Z.; Smith, G. R.; Hochstrasser, R. M. *Chem. Phys. Lett.* **1991**, *185*, 179. (d) Palit, D. K.; Ghosh, H. N.; Pal, H.; Sapre, A. V.; Mittal, J. P.; Seshadri, R.; Rao, C. N. R. *Chem. Phys. Lett.* **1992**, *198*, 113. (e) Ghosh, H. N.; Pal, H.; Sapre, A. V.; Mittal, J. P. *J. Am. Chem. Soc.* **1993**, *115*, 11722. (f) Kamat, P. V.; Bedja, I.; Hotchandani, S. *J. Phys. Chem.* **1994**, *98*, 9137. (g) Foote, C. S. *Top. Curr. Chem.* **1994**, *169*, 347. (h) Kamat, P. V.; Guldi, D. M. In *Recent Advances in the Chemistry and Physics of Fullerenes and Related Materials*; Kadish, K. M., Ruoff, R. S., Eds.; The Electrochemical Society: Pennington, NJ, 1996; p 254, and references therein.

(20) (a) Guldi, D. M.; Huie, R. E.; Neta, P.; Hungerbühler, H.; Asmus, K.-D. *Chem. Phys. Lett.* **1994**, *223*, 511. (b) Michaeli, S.; Meiklyar, V.; Levanon, H. In *Recent Advances in the Chemistry and Physics of Fullerenes and Related Materials*; Kadish, K. M., Ruoff, R. S., Eds.; The Electrochemical Society: Pennington, NJ, 1995; p 457.

(21) (a) Nadtochenko, V. A.; Denisov, N. N.; Rubtsov, I. V.; Lobach, A. S.; Moravski, A. P. *Chem. Phys. Lett.* **1993**, *208*, 431. (b) Steren, C. A.; Levstein, P. R.; van Willigen, H.; Linschitz, H.; Biczok, L. *Chem. Phys. Lett.* **1993**, *204*, 23. (c) Michaeli, S.; Meiklyar, V.; Schulz, M.; Möbius, K.; Levanon, H. *J. Phys. Chem.* **1994**, *98*, 7444.

(22) (a) Tanigaki, K.; Ebbesen, T. W.; Kuroshima, S. *Chem. Phys. Lett.* **1991**, *185*, 189. (b) Gevaert, M.; Kamat, P. V. *J. Phys. Chem.* **1992**, *96*, 9883. (c) Dimitrijevic, N. M.; Kamat, P. V. *J. Phys. Chem.* **1993**, *97*, 7623.

(23) (a) Baxendale, J. H.; Wardman, P. *Trans. Faraday Soc.* **1971**, *67*, 2997. (b) Kira, A.; Thomas, J. K. *J. Phys. Chem.* **1974**, *78*, 196. (c) Dimitrijevic, N. M.; Kamat, P. V. *J. Phys. Chem.* **1992**, *96*, 4811.

(24) Balzani, V.; Boletta, F.; Gandolfi, M. T.; Maestri, M. *Top. Curr. Chem.* **1978**, *75*, 1, and references therein.